Innovative: International Multi-disciplinary Journal of Applied Technology
(ISSN 2995-486X) VOLUME 03 ISSUE 02, 2025

Formatıon of Jarosıte Durıng Bacterıal Oxıdatıon of Sulfide Mınerals

Karshieva M.S., Sharipov S.Sh., Danakulova R.A.
Navoi state university of mining and technologies

.

Abstract:

The formation of jarosite-group minerals during bacterial oxidation of sulfide minerals is a common but insufficiently controlled phenomenon in biohydrometallurgical systems. In this study, jarosite precipitation is analyzed as a consequence of redox-driven iron cycling under acidic conditions typical for biooxidation processes. Particular attention is paid to the role of solution Eh–pH parameters, Fe^{3+} activity, and mineral surface evolution during oxidation. Experimental observations demonstrate that jarosite formation is not a direct biological process, but rather a chemically induced mineral transformation triggered by microbially maintained oxidizing conditions. The results show that jarosite precipitation significantly modifies the mineralogical composition of solid residues and affects the kinetics of sulfide oxidation by forming passivating surface layers. The obtained data provide a basis for controlled management of jarosite formation in biooxidation and bioleaching systems.

Key words: *jarosite, bacterial oxidation, Eh–pH control, biooxidation, sulfide minerals, iron cycling.*

Introduction

Bacterial oxidation of sulfide minerals represents a key stage in the processing of refractory ores and concentrates, particularly in biooxidation and bioleaching technologies. In such systems, the oxidation of sulfide minerals proceeds predominantly through an indirect mechanism, where ferric iron acts as the main oxidizing agent, while acidophilic microorganisms regenerate Fe^{3+} from Fe^{2+} under acidic conditions. This concept has been well established in fundamental studies of biohydrometallurgical processes and iron cycling in acidic environments [1–3].

Under low pH conditions, the abiotic oxidation of ferrous iron is kinetically hindered, whereas iron-oxidizing microorganisms significantly accelerate this process by maintaining high redox potentials in solution. As a result, biooxidation systems are typically characterized by elevated Eh

values and high concentrations of ferric iron, which strongly influence both sulfide oxidation kinetics and secondary mineral formation [4,5].

One of the most common mineralogical consequences of prolonged ferric iron accumulation in sulfate-rich acidic solutions is the precipitation of jarosite-group minerals. Jarosite, with the general formula $MFe_3(SO_4)_2(OH)_6$ (where $M = K^+$, Na^+, NH_4^+ or H_3O^+), is thermodynamically stable under strongly oxidizing and acidic conditions and has been widely reported in acid mine drainage systems, acid sulfate soils, and biooxidation residues [6–8]. Its formation is controlled primarily by solution chemistry, particularly pH, redox potential, sulfate activity, and the availability of monovalent cations.

Previous studies have shown that jarosite precipitation plays a dual role in biooxidation systems. On the one hand, jarosite acts as a sink for ferric iron and can incorporate or adsorb potentially toxic elements such as arsenic and lead, thereby influencing metal mobility in acidic environments [9,10]. On the other hand, jarosite commonly forms dense coatings on sulfide mineral surfaces, which restrict mass transfer and reduce the effective rate of oxidation and subsequent metal recovery [11,12].

Despite the extensive literature on jarosite chemistry and environmental occurrence, its formation during bacterial oxidation is often described as a secondary or undesirable side effect rather than as an intrinsic component of the redox-controlled biooxidation system. In many studies, biological activity and mineral precipitation are not clearly distinguished, leading to ambiguity regarding the role of microorganisms in jarosite formation.

The present study considers jarosite formation as a chemically driven process induced by microbially sustained oxidizing conditions. Particular emphasis is placed on the relationship between Eh–pH evolution, ferric iron activity, and mineralogical transformations during bacterial oxidation of sulfide minerals. Such an approach allows jarosite precipitation to be interpreted not merely as a by-product, but as an indicator of redox imbalance and iron supersaturation in biooxidation systems.

II. Objects and methods of research

Bacterial oxidation experiments were conducted using sulfide mineral samples representative of refractory ores. The biooxidation medium was maintained in the strongly acidic range (pH 1.09–2.0) and continuously aerated to ensure oxidizing conditions. Acidophilic iron-oxidizing microorganisms were used to sustain high redox potentials throughout the experiments.

Control of Eh–pH parameters

Redox potential (Eh) and pH were monitored continuously. During active biooxidation, Eh values exceeded 650–700 mV (Ag/AgCl), indicating dominance of ferric iron in solution. Such conditions correspond to the stability field of ferric hydroxy-sulfates according to Fe–S–O–H system diagrams.

Analytical methods

The solid residues formed during oxidation were periodically sampled and analyzed using:

- X-ray diffraction (XRD) for phase identification,
- chemical analysis of iron species in solution.

The evolution of mineral phases was correlated with solution chemistry and redox conditions.

III. Results and their discussion

The bacterial oxidation process is characterized by rapid regeneration of Fe^{3+} through microbial oxidation of Fe^{2+}. When ferric iron accumulates in acidic sulfate solutions, hydrolysis reactions

become thermodynamically favorable. Under such conditions, jarosite precipitation proceeds according to the generalized reaction:

$$M^{+} + 3Fe^{3+} + 2SO_4^{2-} + 6H_2O \rightarrow MFe_3(SO_4)_2(OH)_6 + 6H^{+}$$

This reaction results in additional proton release, which stabilizes the acidic environment and suppresses neutralization effects. Importantly, microorganisms do not directly participate in jarosite crystallization; their role is limited to maintaining high Eh values that enable ferric iron supersaturation.

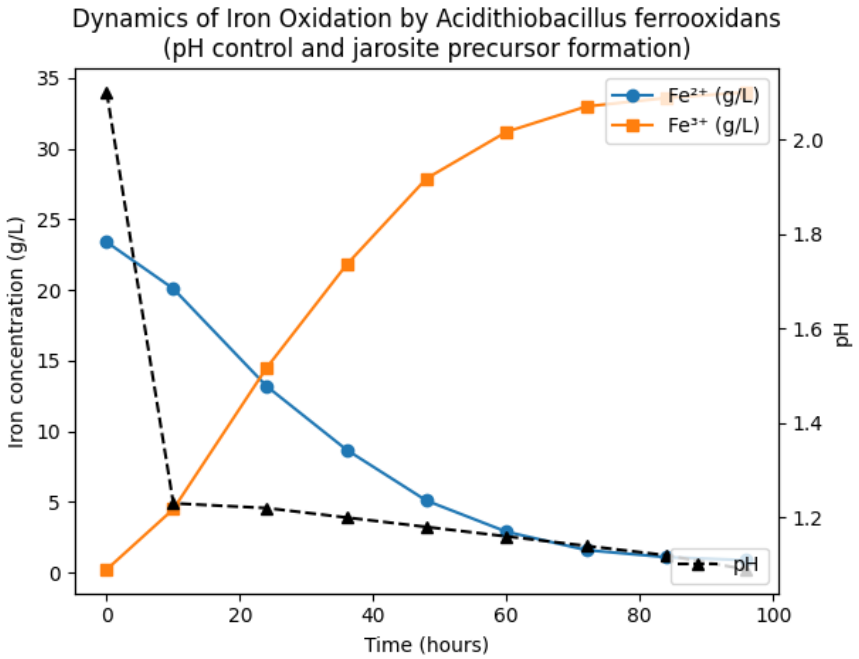

Figure 1. Dynamics of iron oxidation by Acidithiobacillus ferrooxidans showing Fe^{2+} depletion, Fe^{3+} accumulation, and pH changes over time.

The figure illustrates the coupled evolution of ferrous iron, ferric iron, and pH during bacterial oxidation by *Acidithiobacillus ferrooxidans* over a 96 h period. The process can be clearly divided into three kinetically and geochemically distinct stages.

Initial Stage (0–10 h): Acidification and Onset of Iron Oxidation

At the beginning of the experiment, the solution pH is relatively high (pH ≈ 2.10), while the concentration of Fe^{2+} is maximal (23.4 g/L) and Fe^{3+} is present only in trace amounts (0.23 g/L). During the first 10 h, a sharp decrease in pH to approximately 1.23 is observed. This rapid acidification is attributed to the initiation of microbial oxidation of ferrous iron and the associated proton-generating reactions.

At this stage, iron oxidation is already detectable, but the system has not yet reached ferric iron dominance. The rapid drop in pH reflects the transition from an initially metastable acidic solution to a strongly acidic biooxidation regime. Importantly, this early acidification precedes significant jarosite formation and primarily reflects redox-driven acid generation rather than mineral precipitation.

Intermediate Stage (10–48 h): Establishment of Ferric Iron Dominance

After 10 h, the pH stabilizes within a narrow range between 1.09 and 1.23, indicating the establishment of a buffered acidic system. This stabilization coincides with a pronounced decrease in

Fe^{2+} concentration from 20.1 to 5.1 g/L and a simultaneous increase in Fe^{3+} concentration from 4.5 to approximately 27.9 g/L.

This stage represents the most active period of microbial iron oxidation. The sustained low pH and continuous accumulation of ferric iron indicate that *A. ferrooxidans* efficiently regenerates Fe^{3+}, maintaining high redox potentials. From a thermodynamic perspective, these conditions correspond to the stability field of ferric hydroxy-sulfate phases, including jarosite.

The near-constant pH despite ongoing proton generation suggests buffering by ferric iron hydrolysis and the formation of poorly ordered ferric sulfate precursors. This behavior confirms that jarosite formation is initiated indirectly as a chemical response to ferric iron supersaturation rather than as a biologically controlled process.

Late Stage (48–96 h): Iron Supersaturation and Jarosite Precursor Formation

During the final stage of the experiment, Fe^{2+} concentration decreases to residual levels (0.89 g/L), while Fe^{3+} approaches a plateau at approximately 34 g/L. The pH remains stably within the range 1.09–1.12, demonstrating a strongly acidic and highly oxidizing environment.

Such conditions are characteristic of ferric iron supersaturation and are favorable for the nucleation and growth of jarosite-group minerals. The plateauing of Fe^{3+} concentration indicates that the rate of ferric iron generation becomes balanced by precipitation processes, including jarosite precursor formation.

Mineralogically, this stage is expected to correspond to the development of ferric sulfate coatings on sulfide mineral surfaces. These coatings progressively limit mass transfer, leading to a gradual transition from reaction-controlled to diffusion-controlled oxidation kinetics.

Overall Implications for Biooxidation Systems

The combined evolution of iron speciation and pH clearly demonstrates that jarosite formation is a redox-controlled phenomenon governed by ferric iron accumulation under strongly acidic conditions. Microbial activity plays a crucial indirect role by sustaining high redox potentials, while the actual precipitation of jarosite is driven by solution chemistry.

From a process standpoint, the figure highlights the dual role of jarosite formation. While it contributes to chemical stabilization of the system by buffering pH and immobilizing ferric iron, excessive accumulation may negatively affect biooxidation efficiency by passivating mineral surfaces.

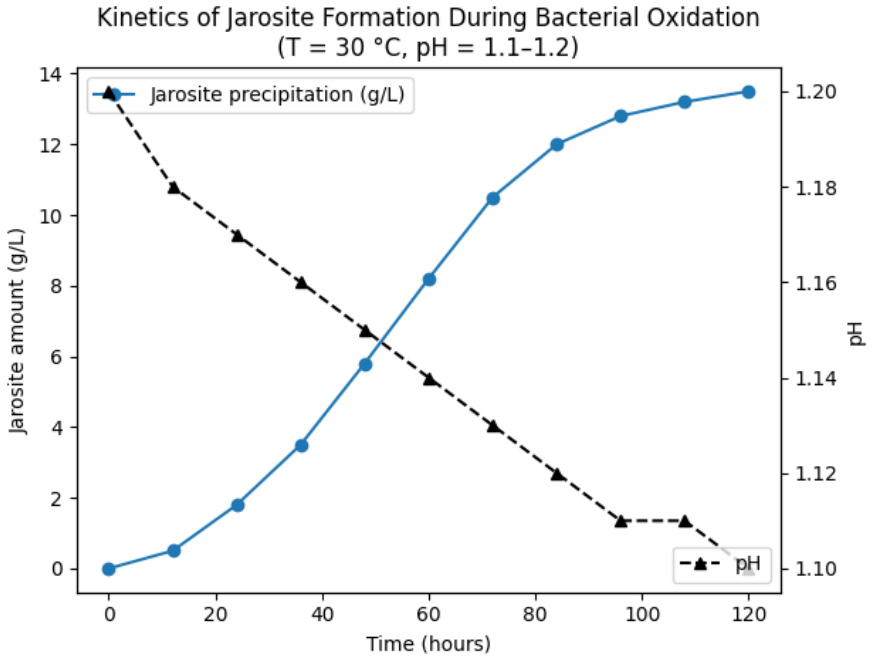

Figure 2. Kinetics of jarosite formation

The figure shows the temporal evolution of jarosite precipitation during bacterial oxidation at 30 °C under strongly acidic conditions. Jarosite formation proceeds progressively over the entire experimental period, reaching approximately 13.5 g/L after 120 h. The kinetic curve indicates a non-linear behavior, suggesting that jarosite precipitation is controlled by both nucleation and subsequent crystal growth processes.

During the initial stage (0–24 h), jarosite formation is limited, indicating the presence of an induction period associated with ferric iron accumulation and supersaturation. Once sufficient ferric iron activity is achieved, the rate of jarosite precipitation increases markedly between 24 and 72 h. This stage corresponds to active nucleation and growth of jarosite under stable acidic conditions.

After approximately 72 h, the precipitation rate decreases and the jarosite concentration approaches a plateau. This behavior indicates that the system reaches a quasi-steady state, where the rate of ferric iron generation becomes balanced by its consumption through jarosite formation.

Throughout the entire experiment, the pH remains within a narrow range of 1.1–1.2. Such pH stability is characteristic of jarosite-forming systems and reflects effective buffering by ferric iron hydrolysis and sulfate complexation. The absence of significant pH fluctuations confirms that jarosite precipitation occurs under chemically controlled conditions rather than being driven by external pH adjustments.

The close temporal correlation between stable pH and increasing jarosite concentration demonstrates that jarosite formation is governed primarily by ferric iron supersaturation under strongly acidic conditions. Microbial activity plays an indirect role by sustaining oxidizing conditions, while the precipitation process itself is controlled by solution chemistry.

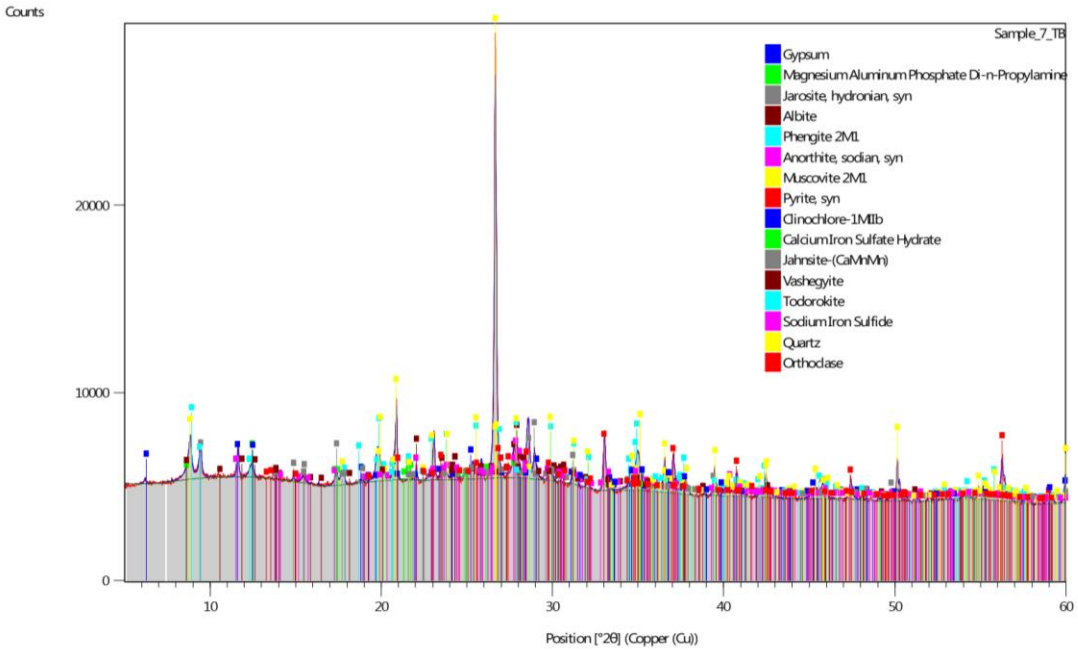

Figure 3. X-ray diffraction pattern of jarosite formed during bacterial oxidation of sulfide minerals.

The X-ray diffraction (XRD) pattern of the solid residue obtained after bacterial oxidation reveals a complex multiphase mineral assemblage, reflecting intensive chemical and mineralogical transformations under strongly acidic and oxidizing conditions. Among the identified phases, particular attention is given to the presence of jarosite-group minerals, which represent a key secondary phase formed during the process.

Distinct diffraction peaks corresponding to hydronium jarosite ($H_3OFe_3(SO_4)_2(OH)_6$) are clearly observed in the pattern. These reflections are consistent with characteristic jarosite peaks typically appearing in the 2θ range of approximately 15–35° (Cu Kα radiation), confirming the formation of jarosite under the applied biooxidation conditions. The presence of hydronium jarosite rather than potassium- or sodium-dominated jarosite indicates formation in a strongly acidic environment with limited availability of alkali cations, which is typical for bacterial oxidation systems operating at low pH.

The intensity and sharpness of the jarosite reflections suggest that jarosite is not merely present as an amorphous or poorly ordered phase, but occurs as a crystalline mineral. This observation is consistent with prolonged exposure of the system to high ferric iron concentrations and sustained redox potentials, which favor nucleation and growth of jarosite rather than transient ferric hydroxysulfate phases.

In addition to jarosite, gypsum and iron sulfate hydrate phases are detected, indicating high sulfate activity in solution during oxidation. The coexistence of jarosite with gypsum reflects the advanced stage of sulfate accumulation and confirms that the system evolved toward a sulfate-dominated geochemical regime. Importantly, the simultaneous presence of quartz, feldspars (albite, anorthite, orthoclase), and mica phases (muscovite, phengite) suggests that these silicate minerals are

largely inherited from the original material and remain relatively stable under the experimental conditions.

The absence of significant peaks corresponding to ferrihydrite or goethite is notable and indicates that iron precipitation proceeds preferentially through the jarosite pathway rather than through formation of iron oxyhydroxides. This is in agreement with the low pH conditions (≈1.1–1.2) maintained during the experiment, which thermodynamically suppress the stability of Fe(III) oxyhydroxides and favor jarosite-group minerals.

Residual sulfide phases, such as pyrite, are still detected in minor amounts, suggesting incomplete oxidation of primary sulfides. However, the presence of jarosite coatings inferred from the XRD data supports the conclusion that secondary ferric sulfate minerals contribute to surface passivation of sulfide grains, which may limit further oxidation at advanced stages of the process.

Overall, the XRD results confirm that jarosite formation is a dominant mineralogical outcome of bacterial oxidation under strongly acidic and oxidizing conditions. The formation of crystalline jarosite reflects ferric iron supersaturation and sustained low pH, and provides direct mineralogical evidence supporting the kinetic and chemical interpretations derived from solution chemistry and pH evolution data.

IV. CONCLUSION AND FUTURE WORK

Based on the results obtained in this study, the following conclusions can be drawn.

1. Bacterial oxidation of sulfide minerals under strongly acidic conditions leads to intensive regeneration of ferric iron and establishment of high redox potentials, creating favorable conditions for the formation of jarosite-group minerals.

2. Jarosite formation was shown to be a chemically driven process induced by ferric iron supersaturation in sulfate-rich acidic solutions, rather than a direct result of microbial metabolism. The role of microorganisms is indirect and limited to sustaining oxidizing conditions through continuous Fe^{2+} oxidation.

3. The evolution of pH within a narrow range of 1.09–1.23 during the main oxidation stage corresponds to the thermodynamic stability field of jarosite and suppresses the formation of ferric oxyhydroxides, promoting precipitation of ferric hydroxy-sulfates.

4. Kinetic analysis indicates the presence of an induction period followed by an accelerated stage of jarosite precipitation and a subsequent quasi-steady state, suggesting a transition from nucleation-controlled to growth-controlled precipitation mechanisms.

5. X-ray diffraction analysis confirmed the formation of crystalline hydronium jarosite as a dominant secondary phase, indicating prolonged exposure of the system to high ferric iron activity and strongly acidic conditions.

6. The formation of jarosite contributes to mineral surface passivation, which may limit further oxidation of residual sulfide minerals at advanced stages of the process and influence overall biooxidation efficiency.

7. The obtained results demonstrate that jarosite formation can serve as a mineralogical indicator of redox imbalance and ferric iron supersaturation in biooxidation systems, providing a basis for controlled regulation of process conditions in biohydrometallurgical operations.

REFERENCES

1. Rawlings D.E. Characteristics and adaptability of iron- and sulfur-oxidizing microorganisms used for the recovery of metals from minerals. Microbial Cell Factories, 2005.
2. Sand W., Gehrke T., Jozsa P.G., Schippers A. (Bio)chemistry of bacterial leaching — direct vs. indirect mechanisms. Hydrometallurgy, 2001.
3. Rohwerder T., Gehrke T., Kinzler K., Sand W. Bioleaching review. Applied Microbiology and Biotechnology, 2003.
4. Singer P.C., Stumm W. Acidic mine drainage: the rate-determining step. Science, 1970.
5. Nordstrom D.K., Alpers C.N. Geochemistry of acid mine waters. Reviews in Economic Geology, 1999.
6. Dutrizac J.E., Jambor J.L. Jarosites and their application in hydrometallurgy. Reviews in Mineralogy, 2000.
7. Baron D., Palmer C.D. Solubility of jarosite at 4–35 °C. Geochimica et Cosmochimica Acta, 1996.
8. Bigham J.M., Nordstrom D.K. Iron and aluminum hydroxysulfates from acid sulfate waters. Reviews in Mineralogy, 2000.
9. Acero P., Ayora C., Torrento C., Nieto J.M. Trace element behavior during jarosite precipitation. Geochimica et Cosmochimica Acta, 2006.
10. Savage K.S., Tingle T.N., O'Day P.A., Waychunas G.A., Bird D.K. Arsenic speciation in jarosite. American Mineralogist, 2000.
11. Sasaki K., Konno H. Morphology of jarosite-group compounds precipitated from biologically oxidized iron solutions. Canadian Mineralogist, 2000.
12. Dutrizac J.E. The effect of jarosite formation on iron control in hydrometallurgical processes. Hydrometallurgy, 1983.